INSTITUTE OF PHYSICS PUBLISHING and INTERNATIONAL ATOMIC ENERGY AGENCY NUCLEAR FUSION

Nucl. Fusion **45** (2005) 1386–1395 doi:10.1088/0029-5515/45/11/020

Study of lower hybrid current drive efficiency over a wide range of FTU plasma parameters

V. Pericoli Ridolfini, G. Calabrò, L. Panaccione, FTU team and ECH team[1]

Associazione EURATOM-ENEA sulla Fusione, Via E. Fermi 45, 00044 Frascati (Roma), Italy
[1] Associazione EURATOM-ENEA-CNR sulla Fusione, IFP-CNR, Via R. Cozzi 53, 20125 Milano, Italy

E-mail: pericoli@frascati.enea.it

Received 17 January 2005, accepted for publication 1 August 2005
Published 25 October 2005
Online at stacks.iop.org/NF/45/1386

Abstract

The key quantities affecting the efficiency of Lower Hybrid (LH) radiofrequency waves in driving non-inductively the toroidal current in a tokamak have been recognized by means of a linear regression analysis over all the data available for the Frascati Tokamak Upgrade. The parameter space is bounded within the following ranges: line averaged plasma density $0.29 \times 10^{20} \leqslant \bar{n}_e \leqslant 1.29 \times 10^{20}\,\mathrm{m}^{-3}$, central electron temperatures $1.1 \leqslant T_{e0} \leqslant 7.4\,\mathrm{keV}$, corresponding to volume averaged temperatures $0.27 \leqslant \langle T_e \rangle \leqslant 1.2\,\mathrm{keV}$, plasma current $0.3 \leqslant I_p \leqslant 0.7\,\mathrm{MA}$, magnetic field $4 \leqslant B_{T0} \leqslant 7.2\,\mathrm{T}$, with a safety factor between $4.7 \leqslant q_a \leqslant 10.7$, LH power $0.4 \leqslant P_{LH} \leqslant 2.1\,\mathrm{MW}$ and LH parallel refraction index $1.32 \leqslant N_{\|0} \leqslant 2.42$. The experimental current drive (CD) efficiency, reduced to the effective ion charge state $Z_{eff} = 1$, varies for this data set within $0.12 \leqslant \eta^*_{CD} \leqslant 0.34\,\mathrm{A\,W^{-1}} \times 10^{20}\,\mathrm{m}^{-2}$. A linear regression analysis gives a reliable scaling law for η^*_{CD} with a correlation coefficient close to 0.9 that points out the importance of the various quantities. The CD efficiency is a significantly increasing function of $\langle T_e \rangle$ and B_T, and a decreasing one of q_a and P_{LH}, while $N_\|$ and $\bar{n}_e$ have limited influence. The physical reasons for the observed trend related to the variation of each parameter are recognized and discussed. The main causes are identified in the modification suffered by the $N_\|$ spectrum along the ray trajectory before the power can be absorbed by the electrons and in the interaction with the edge plasma density fluctuations. The analysis also allows putting into evidence the synergy between the LH and electron cyclotron waves, when the latter are absorbed directly on the LH generated suprathermal electron tails and produce the highest values of η^*_{CD}.

PACS numbers: 52.55.Wq, 52.50.Sw

(Some figures in this article are in colour only in the electronic version)

1. Introduction

The efficiency of the lower hybrid (LH) waves in driving toroidal currents in tokamaks is a key issue for dimensioning an LH system for ITER. Its magnitude, however, shows a large variability, according to published data, as reported in [1] and references therein. It can exceed a factor of 3, when comparing different tokamaks, and even a factor of 2 for a single device, e.g. Frascati Tokamak Upgrade (FTU). The volume averaged electron temperature $\langle T_e \rangle$ was recognized in that paper to be the macroscopic plasma parameter that mostly affects the current drive (CD) efficiency, η_{CD}, but it cannot explain alone the large scattering of the experimental data, except when its variation largely prevails over that of the other quantities.

These considerations prompted us to start a multi-parameters analysis for the lower hybrid CD (LHCD) efficiency, exploiting the large amount of data so far collected in FTU in a quite wide volume in the space of the main plasma variables. The first purpose was to single out those physical factors, common to all tokamaks, that could deserve more investigations by other LH teams, through either experiments or modelling of the LH waves–plasma interaction. This study aims to be the starting point for building a database in order to arrive at scaling laws independent of the particular tokamak.

Table 1. Main parameters of the three RF systems of FTU.

	LHCD (lower hybrid current drive)	ECH (electron cyclotron heating)	IBW (ion Bernstein waves)
Frequency	8 GHz	140 GHz	433 MHz
Nominal unit power per tube (on load)	1 MW	0.5 MW	0.5 MW
Pulse length	1 s	0.5 s	1 s
Number of tubes	6 gyrotrons	4 gyrotrons	2 klystrons
Launcher type	Phased array of 4 × 12 waveguides per structure	Mirror system	2 waveguide system
Maximum launched power on plasma	2.2 MW (10 MW m^{-2})	1.5 MW	0.4 MW

A second goal was to develop a useful tool for future FTU experiments. Here, then, we refine the analysis of the LHCD existing data, the most recent summary of which can be found in [2] but do not present particularly new LHCD results or performances, either technical or physical.

The LHCD physics is of worldwide interest since this technique is exploited at present on many tokamaks such as JET in the European Union, JT-60U and TRIAM-1M in Japan, HT-7 in China, Tore Supra in France, or in the past on PLT, PBX and Alcator-C (USA), TdeV (Canada), Asdex (Germany), JT-60 (Japan); while it is planned in the short term in the existing devices Alcator C-mod (USA) and SST-1 (India), and in the tokamaks under construction in China (EAST) and South Korea (KSTAR). In this wide panorama of machines FTU characterizes as a medium size compact high-field/high-density tokamak with major radius $R_0 = 0.935$ m, minor radius $a = 0.3$ m, toroidal magnetic field at the vessel centre $B_{T0} \leqslant 8$ T, plasma line averaged density $\bar{n}_e \leqslant 4 \times 10^{20}$ m^{-3} and maximum plasma current $I_p \leqslant 1.6$ MA. Additional heating is applied only through three different radiofrequency (RF) systems, whose main parameters are summarized in table 1. In addition to LHCD we will deal only with electron cyclotron heating (ECH) throughout this paper. Further details on the FTU device can be found in [3].

This paper is arranged as follows: in section 2 we present the FTU database, the criteria for the data selection and the kind of analysis performed; in section 3 we illustrate the main results that are discussed in section 4; section 5 is devoted to the interesting case of the ECH power being directly absorbed by the fast electron (e$^-$) tails generated by the LH waves, and finally in section 6 we give our conclusions.

2. Data handling and screening

The parameter space spanned presently by LHCD data on FTU is bounded within the following limits: line averaged plasma density $0.29 \times 10^{20} \leqslant \bar{n}_e \leqslant 1.29 \times 10^{20}$ m^{-3}, central electron temperatures $1.1 \leqslant T_{e0} \leqslant 7.4$ keV, corresponding to volume averaged temperatures between $0.27 \leqslant \langle T_e \rangle \leqslant 1.2$ keV, plasma current $0.3 \leqslant I_p \leqslant 0.7$ MA, toroidal magnetic field $4 \leqslant B_{T0} \leqslant 7.2$ T, corresponding to an edge safety factor between $4.7 \leqslant q_a \leqslant 10.7$ (the approximate relation $q_a = 0.53 \times B_{T0}(\mathrm{T})/I_p(\mathrm{MA})$ holds in FTU) and effective ion charge state $1.1 \leqslant Z_{eff} \leqslant 9$. For the rest of this paper, however, cases with $Z_{eff} > 6$ are completely neglected. In figure 1 we present the data points distribution as a function of $\bar{n}_e$ only, for the fraction of the driven current (see below for the details on its evaluation) in frame (*a*); for the volume electron temperature $\langle T_e \rangle$ in frame (*b*); for the plasma current in frame (*c*); for the safety factor at the edge in frame (*d*) and for the average ion charge state in frame (*e*). Circles and crosses single out discharges, respectively, with $I_{LH}/I_p > 0.7$, for which the loop voltage V_{loop} is always $\leqslant$0.2 V, and $0.5 \leqslant I_{LH}/I_p \leqslant 0.7$, with V_{loop} always <0.45 V, that have been selected for the present analysis whereas dots refer to the other discharges. The ranges of the RF parameters are instead the following: coupled LH power $0.4 \leqslant P_{LH} \leqslant 2.1$ MW, with peak value of the launched $N_\parallel$ spectrum ($N_\parallel$ is the parallel index of refraction) $1.32 \leqslant N_{\parallel 0} \leqslant 2.42$ and ECH coupled power $0 \leqslant P_{ECH} \leqslant 0.8$ MW. The hypervolume of the parameter space filled by the data is large enough for a significant statistical analysis to be carried out. A distinction will be made throughout this paper between whether the ECH power is absorbed on the bulk electrons, which is the usual way of operation in most tokamaks, or directly on the fast e$^-$ tails generated by the LH waves. Indeed, in this second case peculiar effects can be produced, as reported first for a tokamak plasma in previous works on FTU [4, 5].

To obtain solid results from the analysis we adopted quite stiff criteria in selecting and handling the data. The quality and reliability of each piece of data eligible for the analysis has been singularly checked carefully. It is also requested that a quasi-steady phase be attained that lasts at least 80 ms, during which the variation of the main quantities must be small enough that an average value can be confidently extracted. In particular, it is important to get rid of inductive effects driven by changes in the current profile to avoid doubtful evaluation of the resistive V_{loop}. Within our goal of 10% accuracy limit, an acceptable steadiness occurs always within 0.12 s from the start of a constant power LH phase. This delay may be considerably shorter than the resistive current relaxation time τ_R ($\tau_R \approx 0.4$ s, when T_{e0} is >6 keV, as it often happens) presumably because the plasma resistivity plays only a minor role close to almost full CD conditions, when the dominant electro-motive force is no more the ohmic (OH) electric field but just the LH waves driving the current locally. In this context, we accept a given discharge if the following limits are not exceeded in the 0.08 s time interval considered. For variations to be ascribed to shifts of the plasma column or to spurious external pick-up that can easily be averaged to zero and have usually a time scale <40 ms $|\Delta V_{loop}|$ must be $\leqslant$0.025 V. The limit is lowered to $|\Delta V_{loop}| \leqslant 0.005$ V if the cause is some plasma current evolution, which shows usually as slow drifts with a time scale $\geqslant$80 ms. The boundaries imposed to the deviation from the average to the other macroscopic

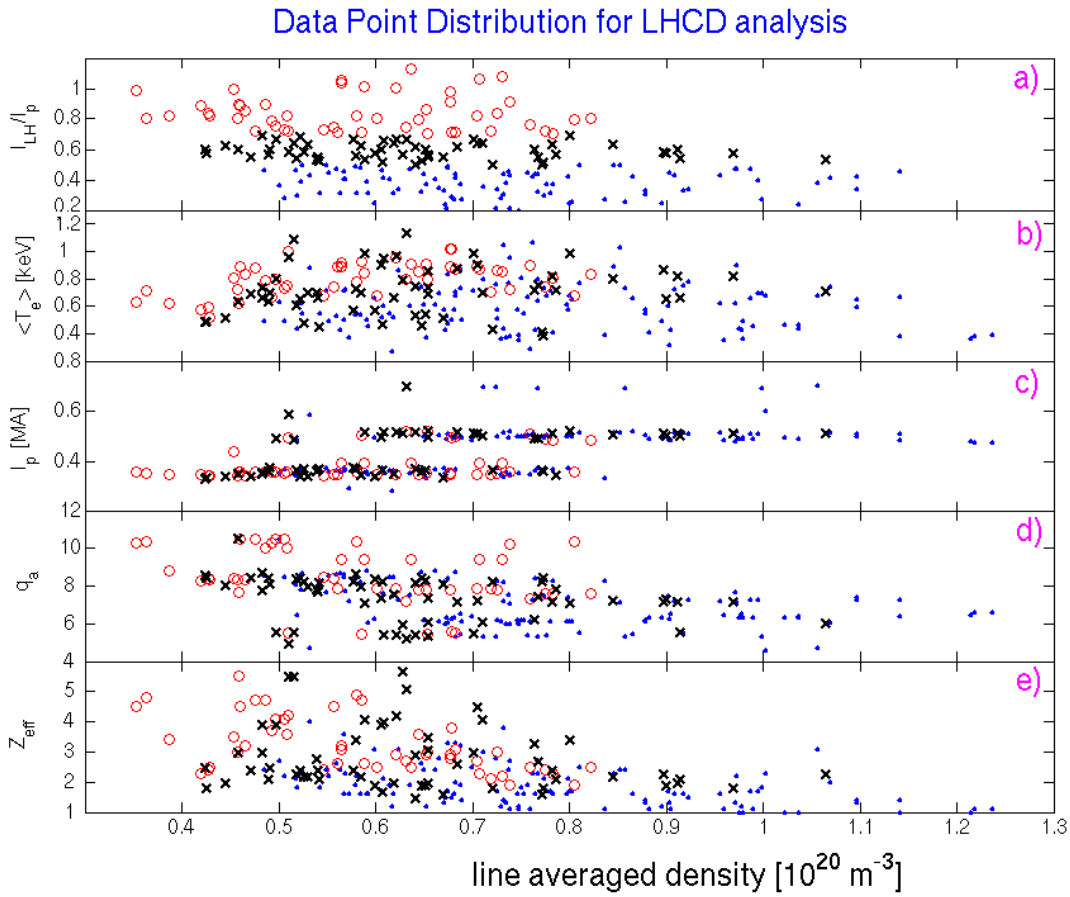

Figure 1. Distribution of the points in the FTU database for LHCD assuming the line averaged density as the free parameter. The analysis has been limited to discharges with $Z_{\rm eff} < 6$ and either with more than 70% of LH driven current (○) or extended also to $50\% < I_{\rm LH}/I_{\rm p} \leqslant 70\%$ (×). The dots (·) refer to all the other discharges.

quantities are: $|\Delta\bar{n}_{\rm e}| \leqslant 0.02 \times 10^{20}\,{\rm m}^{-3}$, $|\Delta Z_{\rm eff}| \leqslant 0.2$, $|\Delta\langle T_{\rm e}\rangle| \leqslant 0.04\,{\rm keV}$. Discharges with large evident MHD activity are rejected, because of the quite fast radial current diffusion and loss of energetic electrons. A doubtless sign of this unwanted activity is a decrease of density during the LH pulse, which instead increases in MHD free discharges due to the large LH induced particle recycling onto the FTU walls [6].

The most frequent criticism of the estimate of the CD efficiency in situations other than full CD is the uncertain contribution of the so-called 'hot ohmic current', $I_{\rm hot}$, i.e. the current driven by the residual OH electric field directly on the LH generated fast e^- tail. The tail anomalous conductivity can build a significant ratio $I_{\rm hot}/I_{\rm LH}$, as shown in [7] and hence produce a large overestimate of the CD efficiency, as in the very long discharges of TRIAM-1M [8]. However in FTU the appropriate conditions, namely simultaneous low collisionality, high loop voltage and low LH power, are met only in quite peculiar cases, as pointed out in a previous work [1], that are excluded from the present analysis. Indeed, the Dreicer electric field for a free acceleration of electrons as fast as a LH wave with $N_\parallel \approx 1.7$ is never $<2.0\,{\rm V}$, whereas the discharges analysed here all have $V_{\rm loop} < 0.45\,{\rm V}$. Nevertheless, to further reduce the effect of the electric field on the results, we first concentrated on a subset of data with the fraction of the RF driven current $I_{\rm LH}/I_{\rm p} > 0.7$, for which $V_{\rm loop} \leqslant 0.2\,{\rm V}$ and $\Delta V_{\rm loop}/V_{\rm loop,OH} \geqslant 80\%$, and then compared the results with those from a data set extended to comprise discharges with $I_{\rm LH}/I_{\rm p} \geqslant 0.5$ and $\Delta V_{\rm loop}/V_{\rm loop,OH} \geqslant 58\%$ to highlight still possible influence of $V_{\rm loop}$. The two subsets comprise, respectively, 44 and 99 points on a total of 289, and both include also over CD regimes, with $I_{\rm LH}/I_{\rm p} \approx 1.13$ and $\Delta V_{\rm loop}/V_{\rm loop,OH} \approx 118\%$. The lack of any significant distinction between the two cases, as detailed below, strongly supports the rightness of our selection criterion. The amount of the LH driven current is deduced from the total current balance:

$$I_{\rm p} = I_{\rm LH} + I_{\rm OH} + I_{\rm boot}. \tag{1}$$

The OH residual fraction is evaluated from the loop voltage drop, taking into account the change of plasma resistivity from OH to LH phase, due to the variation of $\langle T_{\rm e}\rangle$ and $Z_{\rm eff}$, similarly to what was done in [1]:

$$\frac{I_{\rm OH}}{I_{\rm p}} = \frac{V_{\rm l,LH}}{V_{\rm l,OH}} \cdot \frac{\langle T^{3/2}_{\rm e,LH}\rangle}{\langle T^{3/2}_{\rm e,OH}\rangle} \cdot \frac{Z_{\rm eff,OH}}{Z_{\rm eff,LH}}. \tag{2}$$

The bootstrap contribution, $I_{\rm boot}$, is evaluated from the temperature and density profiles according to [9]. In many cases the bootstrap current fraction revealed to be non-negligible within our accuracy limits, since $I_{\rm boot}/I_{\rm LH}$ can exceed 30% when strong $\nabla T_{\rm e}$ are formed in internal transport barrier regimes [6], while for the majority of cases it is in

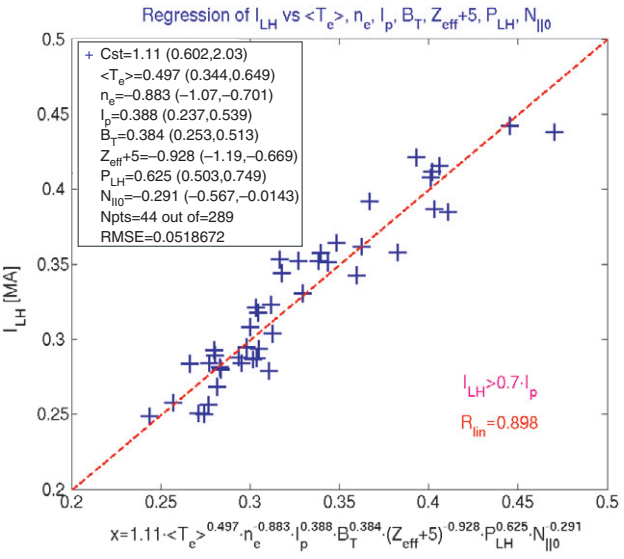

Figure 2. Multiple linear regression analysis for the amount of LH driven current. Only discharges with $Z_{\rm eff} < 6$ and $I_{\rm LH}/I_{\rm p} > 70\%$ are considered. Units are $T_{\rm e}$ (keV), $n_{\rm e}$ (10^{20} m^{-3}), $I_{\rm p}$ (MA), $B_{\rm T}$ (T), $P_{\rm LH}$ (MW).

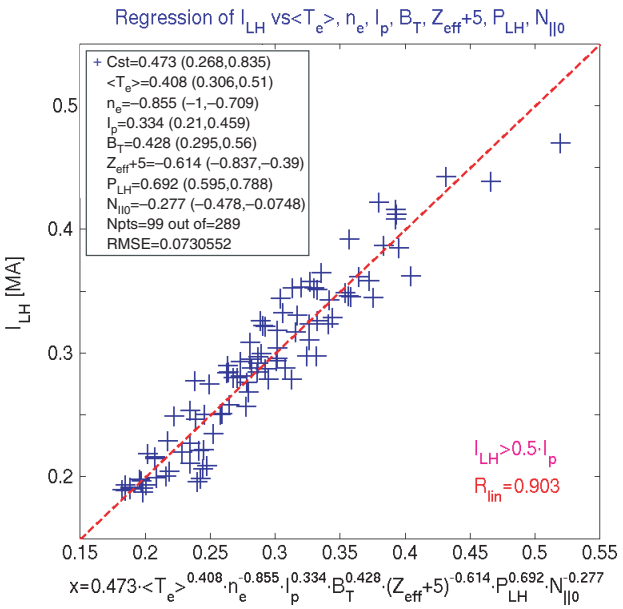

Figure 3. Multiple linear regression analysis for the amount of LH driven current. Only discharges with $Z_{\rm eff} < 6$ and $I_{\rm LH}/I_{\rm p} > 50\%$ are considered. Units are $T_{\rm e}$ (keV), $n_{\rm e}$ (10^{20} m^{-3}), $I_{\rm p}$ (MA), $B_{\rm T}$ (T), $P_{\rm LH}$ (MW).

the range ≈10–20%. The consideration of $I_{\rm boot}$ led to a more ordered data set but lowered a bit the highest FTU values of $\eta_{\rm CD}$ previously quoted [10], when the bootstrap contribution was neglected.

3. Regression analysis results

Regression analysis technique is usually utilized when searching for the relevant weights in a multi-parameter dependence. Here we started directly on the magnitude of $I_{\rm LH}$, rather than on $\eta_{\rm CD}$, which is a derived quantity $\eta_{\rm CD} = \bar{n}_{\rm e} \cdot I_{\rm LH} \cdot R_0/P_{\rm LH}$. The range spanned by $I_{\rm LH}$ values is between 0.25 and 0.45 MA. Discharges with the ECH power absorbed by the thermal bulk electrons are included in the data set, whereas cases where the cold EC resonance is absent and direct absorption can take place only on the LH fast e$^-$ tails are excluded. This choice aims to highlight possible synergetic effects, as detailed in section 5. Many quantities have been taken into account as independent variables, but the only ones that proved to be essential for an acceptable correlation are the following: (a) volume averaged temperature; (b) line averaged density, (c) plasma current, (d) toroidal magnetic field, (e) effective ion charge, (f) LH power and (g) peak value of the launched $N_\parallel$ spectrum. The accessibility of the LH waves to the core plasma plays no relevant role, because all the selected discharges satisfy the good accessibility criterion fixed in [1]: $N_{\parallel 0} - N_{\parallel,\rm acc} \geqslant 0$, $N_{\parallel,\rm acc}$ being the minimum $N_\parallel$ value requested for a LH wave to access a plasma with density $n_{\rm e} = \bar{n}_{\rm e}$ and magnetic field $B = B_{\rm T0}$.

The analysis result is shown in figure 2 where the experimental values of $I_{\rm LH}$ are plotted versus the regression variable. The correlation coefficient $R_{\rm lin}$ is very close to 0.9 and the root mean square deviation is around 5% only. As anticipated, the loop voltage does not play any role; if included in the regression variable it produces $\Delta R_{\rm lin} \approx 0.001$ only, and it is assigned with an exponent ≈0.01. To further support such a statement figure 3 shows the result obtained for the data set enlarged to enclose all discharges with $I_{\rm LH} \geqslant 0.5 \cdot I_{\rm p}$, more than doubling the number of points (99 against 44). The magnitude of all the exponents is substantially confirmed; only that of $(Z_{\rm eff} + 5)$ shows a small decrease from 0.9 to approximately 0.6 but within the error bar of the analysis. In particular, the loop voltage proves once more to be unimportant as many times affirmed for FTU. The multiple linear correlation coefficient remains high, $R_{\rm lin}$ ≈0.9, while the mean deviation increases slightly from 5.2% to 7.3%.

The safety factor q_a of the discharge can be easily included as free parameter instead of either $B_{\rm T0}$ or $I_{\rm p}$, which is linked in FTU by the approximate relation $q_a \approx 0.53 \cdot B_{\rm T0}/I_{\rm p}$, by simply substituting $I^\alpha \cdot B_{\rm T0}^\beta$ with either $0.53^\alpha \cdot q_a^{-\alpha} \cdot B_{\rm T0}^{\beta+\alpha}$ or $0.53^{-\beta} \cdot q_a^\beta \cdot I_{\rm p}^{\alpha+\beta}$. The laws derived are then the following:

$$I_{\rm LH} = 1.11 \cdot \langle T_{\rm e}\rangle^{0.497} \cdot \bar{n}_{\rm e}^{-0.883} \cdot I_{\rm p}^{0.388} \cdot B_{\rm T0}^{0.384} \cdot (Z_{\rm eff} + 5)^{-0.928} \cdot P_{\rm LH}^{0.625} \cdot N_{\parallel 0}^{-0.291} \quad (3a)$$

or

$$I_{\rm LH} = 1.42 \cdot \langle T_{\rm e}\rangle^{0.497} \cdot \bar{n}_{\rm e}^{-0.883} \cdot I_{\rm p}^{0.772} \cdot q_a^{0.384} \cdot (Z_{\rm eff} + 5)^{-0.928} \cdot P_{\rm LH}^{0.625} \cdot N_{\parallel 0}^{-0.291} \quad (3b)$$

or

$$I_{\rm LH} = 0.8676 \cdot \langle T_{\rm e}\rangle^{0.497} \cdot \bar{n}_{\rm e}^{-0.883} \cdot q_a^{-0.388} \cdot B_{\rm T0}^{0.772} \cdot (Z_{\rm eff} + 5)^{-0.928} \cdot P_{\rm LH}^{0.625} \cdot N_{\parallel 0}^{-0.291}. \quad (3c)$$

The measuring units are $I_{\rm LH}$ (MA), $T_{\rm e}$ (keV). $n_{\rm e}$ (10^{20} m^{-3}), $B_{\rm T0}$ (T), $P_{\rm LH}$ (MW). The last formula, equation (3*c*), will be the one more considered throughout this paper. This choice is suggested by the fact that q_a and $B_{\rm T0}$ are physical parameters governing the ray propagation along the plasma radius and the interaction of the LH waves with the plasma edge, as discussed below, while we could not single out so far a clear reason for a direct effect of $I_{\rm p}$.

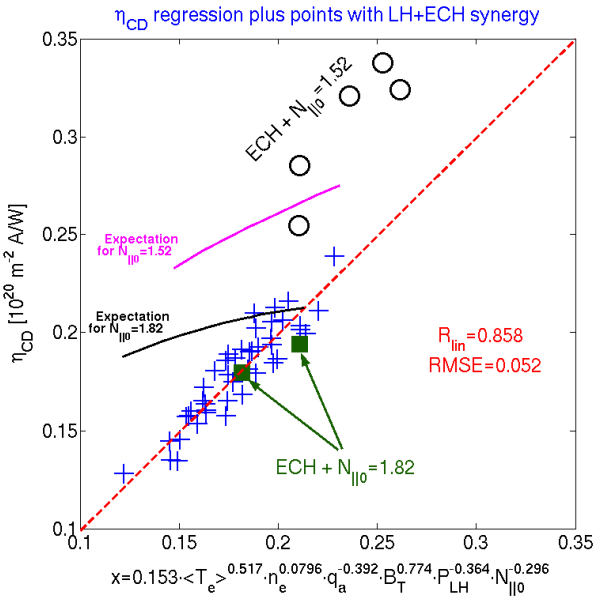

Figure 4. Multiple linear regression analysis for the CD efficiency (done only on the same points of figure 2 represented by +). Values calculated when EC power is also launched and absorption is possible only on the fast e tails are also added. They have $B_T = 7.1\,T$, $I_{LH}/I_p > 50\%$, and $V_{loop} < 0.2\,V$, $N_{\|0} = 1.52$, (O) and $N_{\|0=1.82}$ (■). Very high values of η_{CD} are obtained for $N_{\|0} = 1.52$, despite $\langle T_e\rangle \approx 1.2\,keV$. The two continuous line curves give the average value of the expected CD efficiency for $N_{\|0} = 1.52$ and $N_{\|0} = 1.82$ according to equation (6) for the spanned range of the regression variable.

Equations (3*a*)–(3*c*) show that the linear dependence of I_{LH} on $(Z_{eff} + 5)$, earlier derived in [11], is basically correct. Our choice to fix it to 1 for the rest of the analysis implies a slight modification of the exponents of those variables mainly affecting Z_{eff}, i.e. n_e, P_{LH} and T_e [1, 12]. Applying regression on the CD efficiency calculated for $Z_{eff} = 1$ and defined as in [1], $\eta^*_{CD} = (\bar{n}_e \cdot I_{LH} \cdot R_0)/P_{LH} \cdot (Z_{eff} + 5)/6$, the following scaling law is derived from the same points considered in figure 2:

$$\eta^*_{CD} = 0.1543 \cdot \langle T_e\rangle^{0.517} \cdot \bar{n}_e^{0.0796} \cdot q_a^{-0.393} \cdot B_{T0}^{0.775} \cdot P_{LH}^{-0.364} \cdot N_{\|0}^{-0.296}. \quad (4)$$

The units of η^*_{CD} are $(10^{20}\,m^{-2}\,A\,W^{-1})$, the other units are unchanged. The exponents variation is consistent with the observation that Z_{eff} is in FTU a decreasing function of n_e and an increasing one of T_e and P_{LH}. We always assume 100% absorption of the LH power; therefore this estimate of η^*_{CD} is actually its lower limit. Figure 4, where all the $\eta^*_{CD} (= \eta_{CD}$ at $Z_{eff} = 1)$ values are plotted versus the regression variable, also makes a comparison between the experimental LHCD efficiency and its expected magnitude for two different $N_\|$ spectra, as explained below in section 4. Empty circles single out discharges with EC power injected in the absence of the cold resonance but with possible direct absorption onto the fast e^- tails generated by the LH waves. They have not been included in the regression analysis in order to isolate possible synergetic effects. As highlighted by the figure, these discharges can reveal a very high efficiency with magnitudes up to 0.34 $(10^{20}\,m^{-2}\,A\,W^{-1})$, which can be compared with the best values obtained in JET [13] and JT60-U [14] but at much lower densities and higher electron temperatures ($\bar{n}_e \approx 0.1$–$0.2 \times 10^{20}\,m^{-3}$, $\langle T_e\rangle \approx 2\,keV$). The conditions for this enhancement are discussed in section 5.

A rather high linear correlation coefficient, $R_{lin} \approx 0.86$, is still preserved for the CD efficiency, consistently with figure 2. This large FTU database confirms on a more solid base the statement made more than once, see, e.g. [1], that η_{CD} increases with the electron temperature and it is almost independent of density, for the entire $\bar{n}_e$ range from 0.35 to $1.05 \times 10^{20}\,m^{-3}$. At $\langle T_e\rangle \geqslant 1\,keV$ the magnitude of η^*_{CD} reaches a level close to 0.25 $(10^{20}\,m^{-2}\,A\,W^{-1})$ without any synergy with EC waves. This value is even larger than that expected for $N_{\|0} = 1.82$, approaching the level of $N_{\|0} = 1.52$, and it is quite interesting for ITER that operates in the same density range as FTU.

Effects on η^*_{CD} from some of the variables considered here have been found for other tokamaks also, but the contemporary variation of the other quantities implied in equation (4) is almost never taken into account when comparing different plasmas. The efficiency improvement with $\langle T_e\rangle$ was first noticed by Porkolab [15], further evidenced in JT-60 [16] and JT-60U [17], and confirmed in JET [18]. The increment of η_{CD} with I_p has been observed both in Tore Supra [19] and JT-60U [20], even though it is not considered as the effect of decreasing q_a, a view which we favour instead. The benefit from increasing B_T has been reported for JT-60U [20], but ascribed to the wave accessibility that never plays a significant role here, as remarked above. In this same paper an increment of η_{CD} with $\bar{n}_e$ is also claimed, the only occurrence before the present work. The effect of changing the launched $N_\|$ spectrum has been studied mainly on PLT [21], JT-60U [20] and Asdex [22] with results that usually indicate an enhancement of η_{CD} towards low $N_\|$, larger than that observed in FTU, whereas in JET no significant effect is derived from altering $N_\|$ [23, 24]. To our knowledge, none of the teams involved with LHCD has so far directly identified a negative consequence of increasing the LH power, as instead inferred from equation (4), even though this fact was almost implicit in [25] dealing with the interaction of LH waves with the edge plasma, as detailed in the next section.

4. Discussion

The presence of each variable in the regression and its effect on η_{CD} may be understood on the basis of physical reasons. The magnitude of the exponent instead cannot be predicted from simple arguments, but it would deserve a complex computer modelling of all the phenomena acting on the propagation and absorption of the LH waves.

To discuss the effect on the CD efficiency of the various quantities we should start from the classical definition of CD efficiency [11]:

$$\eta_{CD} = \frac{124}{\ln\Lambda} \cdot \frac{w_2^2 - w_1^2}{\ln(w_2/w_1)} \cdot \frac{1}{5 + Z_{eff}}, \qquad (10^{20}\,m^{-2}\,A\,W^{-1}). \quad (5)$$

Here the hypothesis is made that the LH waves build a fast tail in the electron distribution function bounded within the velocity limits w_1 and w_2, normalized to the speed of light c and with $w_2 > w_1$. According to [26], we further assume that the tail extends on the low velocity side down to where

$w_1 \approx 3.5\, v_{\mathrm{th,e}}/c$ ($v_{\mathrm{th,e}} = (T_\mathrm{e}/m_\mathrm{e})^{0.5}$ is the thermal bulk electron velocity with m_e = electron mass), in order that effective LH absorption by the electrons becomes possible and on the high velocity side up to where $w_2 \equiv v_2/c = 1/N_{\|0}$, reasonably. The following dependence of η_{CD} on T_e then holds:

$$\eta_{\mathrm{CD}} = \frac{7.92}{5 + Z_{\mathrm{eff}}} \cdot \frac{1/N_{\|0}^2 - 2.37 \times 10^{-2} \cdot T_{\mathrm{e,keV}}}{\ln[6.49/(N_{\|0} \cdot \sqrt{T_{\mathrm{e,keV}}})]}, \quad (10^{20}\,\mathrm{m^{-2}\,A\,W^{-1}}). \tag{6}$$

The amount of the driven current, $I_{\mathrm{LH}} = \eta_{\mathrm{CD}} \cdot P_{\mathrm{LH}}/(\bar{n}_\mathrm{e} \cdot R_0)$, is then predicted to increase with $\langle T_\mathrm{e}\rangle$ and to decrease with $N_{\|0}$ and Z_{eff}, besides being directly proportional to P_{LH} and inversely proportional to $\bar{n}_\mathrm{e}$. The predicted increase of η_{CD} with the e^- temperature is similar to that produced by numerical modelling of the ray propagation and absorption carried out in [27]. Our approach is an analytical and simplified description, in terms of $\langle T_\mathrm{e}\rangle$ only, of the upshift of the launched $N_\|$, which in the cited work is instead calculated from the toroidal effects along the ray trajectories, until absorption. Many reflections onto the vessel walls are needed in the model before achieving significant absorption for central e^- temperatures below 10 keV. Another approach to the $N_\|$ spectral change inside the plasma, however, has been recently proposed [28], according to which the LH waves would excite parametric decay instabilities in the very edge of the plasma. These, in turn, would generate a high $N_\|$ tail in the LH power spectrum, so that many passages across the plasma are no more required for the power being fully absorbed.

With respect to the predictions of equation (6), the experimental data instead show that

(a) I_{LH} increases when decreasing q_a (no dependence from equation (6)).
(b) I_{LH} decreases slightly less than linearly when increasing $\bar{n}_\mathrm{e}$.
(c) I_{LH} grows faster with $\langle T_\mathrm{e}\rangle$, close to $\langle T_\mathrm{e}\rangle^{0.5}$, confirming what was reported previously in [1].
(d) I_{LH} grows less than linearly with P_{LH}.
(e) I_{LH} increases remarkably with B_T (no dependence from equation (6)).
(f) I_{LH} increases with $1/N_{\|0}$ much slower.
(g) The dependence on Z_{eff} + 5 is almost inverse linear, consistently with equation (6).

The following discussion provides the physical reasons why the expectations from equation (6) are not fulfilled. The search for quantitative agreement is outside the scope of the present paper and would require to take into account the whole complexity of the system and to have a very reliable tool for calculating the LH radial profile deposition, fast enough to be exploited for quite a large number of cases. To our knowledge no robust numerical exploration has been made so far on purpose for any of the quantities mentioned above, except for $\langle T_\mathrm{e}\rangle$, as already quoted.

The first three features ((a), (b), (c)) may be accounted for by the toroidal upshift of $N_\|$ that the LH waves suffer when propagating in a toroidal geometry. To understand the combined effect of q_a and n_e, we suppose that the effective $N_\|$ spectrum be represented by the $N_{\|0}$ value that the rays acquire at the innermost radius at their first passage, better than by that launched from the LH grill. Indeed, this change along the trajectory unavoidably occurs independently of the subsequent mechanisms of absorption, single or multi-passage, and of filling the gap between the maxwellian electron distribution and the wave velocity. An estimate of this toroidal shift at the first whispering gallery point, where the ray reverts its radial velocity, is derived here in an analytical way from the paper of Barbato and Romanelli [29], and it is plotted in figure 5 as $\Delta N_\|/N_{\|0}$ versus q_a. The ray is supposed to be launched equatorially and two typical FTU densities are considered, namely $\bar{n}_\mathrm{e} = 0.5$ and $0.75 \times 10^{20}\,\mathrm{m^{-3}}$, with q_0, the central value of q, fixed at the most common value for full CD conditions in FTU, i.e. $q_0 = 1.2$. As q_a decreases or n_e increases, the corresponding smaller $N_\|$ upshift implies that the fast e^- tail extends to higher velocities, and hence more current is driven. Figure 5 suggests comparable magnitude of such effects for q_a and n_e, within their range of variability in FTU, whereas equation (3c) assigns more influence to q_a than to n_e, giving them, respectively, the exponents -0.388 and 0.117 only above -1. The reason for the discrepancy is the presence of other counteracting effects of the density, as discussed below, when dealing with the interaction of the LH waves with the edge plasma.

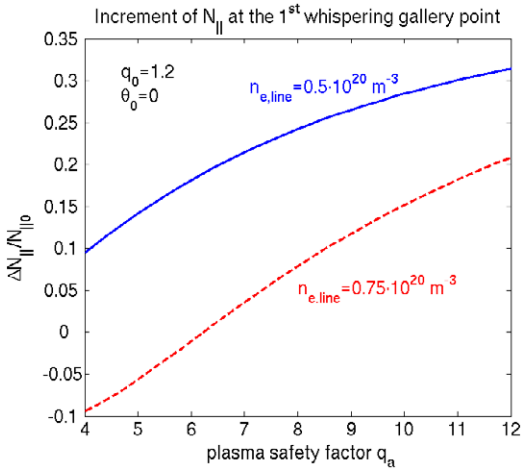

Figure 5. Relative increment of the launched $N_\|$ for an LH wave injected in FTU from the equatorial plane (according to [29]) as a function of the safety factor at the edge for two different plasma densities.

The changes affecting $N_\|$ as rays propagate towards the plasma core together with the conditions for the wave absorption can also account for the fact that the effect of $\langle T_\mathrm{e}\rangle$ on I_{LH}, is larger than that foreseen by equation (6). Indeed, when $\langle T_\mathrm{e}\rangle$ increases, the plasma periphery becomes hotter and rays can be absorbed after a smaller $N_\|$ upshift, i.e. after a lower number of reflections at the walls in a multi-passage absorption scheme. This can be understood by looking at figure 6 that compares the radial profiles of T_e and of the minimum $N_\|$ value required for absorption, $N_{\|,\mathrm{min}} = 3.5 \cdot c/v_{\mathrm{th,e}}$, for the top and the bottom of the $\langle T_\mathrm{e}\rangle$ variability range here considered. The LH absorption region, bounded by $N_{\|,\mathrm{min}}(r)$, is clearly wider in the high temperature case where the point at $N_\| = 4$ is shifted from $r/a = 0$ to $r/a \approx 0.4$. Similar arguments are proposed in [27] when discussing the numerical code estimate of η_{CD} increase with T_{e0} within the 10 keV range.

The divergence from direct proportionality of I_{LH} to P_{LH}, described at the previous point (d), is within the experimental

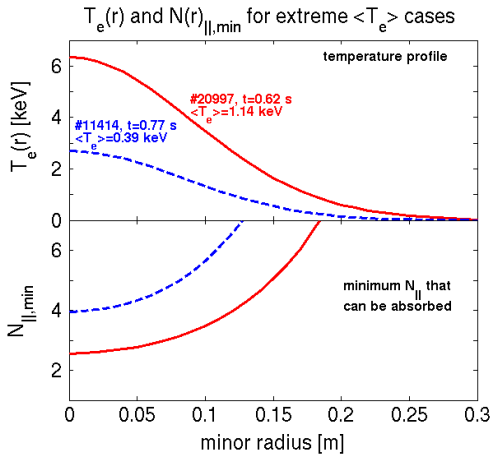

Figure 6. Profiles of e^- temperature (upper) and of the minimum absorbed $N_\parallel$ (lower) for an LH wave in the two extreme cases in terms of $\langle T_e \rangle$ of the data set analysed. Less $N_\parallel$ upshift and hence more prompt absorption occurs in the hotter plasma case.

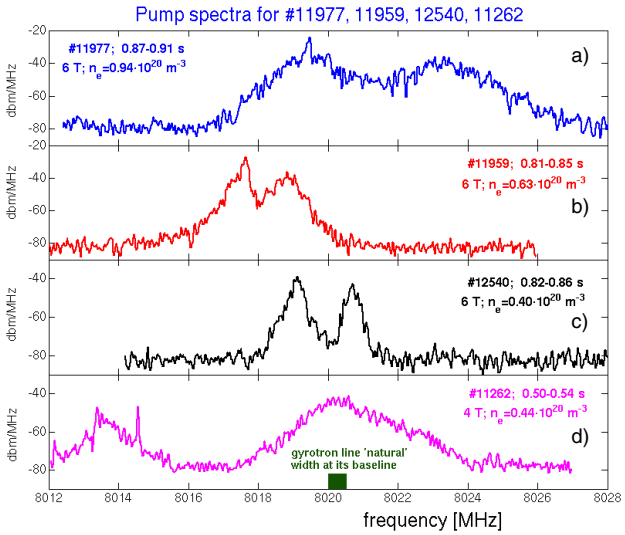

Figure 7. Frequency spectra around the pump frequency for two LH gyrotrons firing simultaneously into FTU. Three different plasma densities and two magnetic fields are considered. The spectral broadening clearly increases with $\bar{n}_e$ and decreases with B_T. The natural width of the main gyrotron emission line is shown as a full box on the bottom frame.

accuracy. If we neglect it and fix the exponent the LH power, equal to 1, the linear correlation coefficient and the data average deviation in the regression would degrade substantially. An exponent smaller than 1 is equivalent to admitting that less effective absorption takes place as power is raised. A possible candidate for that is the modification of the LH wave properties induced by the multiple scattering suffered from density fluctuations at the plasma edge that can degrade η_{CD}, as shown in a previous work [25] on the tokamak Asdex, where $f_{LH} = 2.45\,\text{GHz}$. These processes scatter back part of the incident radiation, which hence is lost, and also give the LH rays a poloidal momentum that spreads the $N_\parallel$ spectrum through the toroidal effects. The most direct evidence of them, the frequency spectral broadening of the LH pump, Δf_{LH}, was in Asdex very well correlated to CD efficiency degradation. Δf_{LH} depends on many plasma quantities; it increases with $\bar{n}_e$ and decreases with B_T. In particular, it is also proportional to the total coupled LH power, since the latter enhances the Scrape-Off Layer (SOL) plasma turbulence.

Evidence of the scattering processes in FTU at much higher f_{LH} ($= 8\,\text{GHz}$), with features very similar to those found for Asdex, is given in figure 7. Here the frequency spectrum detected by an external loop antenna is shown for a time window when two gyrotrons with close frequencies were firing. The first three frames (*a*)–(*c*) refer to discharges with decreasing density and same magnetic field, 6 T, while the last frame (*d*) at $B_{T0} = 4\,\text{T}$ has to be compared with frame (*c*) at very similar densities; clearly the pump spectral width is increasing with $\bar{n}_e$ and decreasing with B_T. Early experiments in FT with the same 8 GHz LH frequency have already confirmed how the pump spectral broadening could be accounted for by the edge wave scattering processes, see [25]. More detailed studies in FTU are made quite difficult by the nature of our LH powers sources. Unlike klystrons, used in Asdex and FT, the gyrotron frequencies are not perfectly stable and never match up with each other, so that the spectra can overlap in a way very difficult to unveil. The main frequency is fixed by the particular setting of the gyrotron control parameters, within an admitted range of about 30 MHz, and at worst may drift $\leqslant 1$ MHz during a single shot about 1 s long. This frequency variability then affects only marginally the spectra shown in figure 7 that are spanned in less than 50 ms. Almost unimportant is also the natural spectral width of the emitted radiation, which is only $\leqslant 0.5$ MHz broad at the spectrum baseline.

The preservation of the main characteristics of the pump spectral broadening then leads to assigning also to the FTU edge density turbulence a role similar to that described in [25] in modifying η_{CD}. The benefit of increasing B_{T0} can be explained by the magnitude of the poloidal kick that the fluctuations give to the radially travelling LH rays, which weakens as B_{T0} rises. The kick amplitude is determined by the ratio of the non-diagonal term of the dielectric tensor $-iD = -i\omega_{pe}^2/(\omega_0\Omega_e)$, which describes the degree of the coupling between the poloidal and radial directions, and the magnitude of the LH wave momentum $k_0 \approx k_\parallel \omega_{pe}/\omega_0$ ($\omega_0 = 2\pi f_{LH}$; $\omega_{pe} = [n_e e^2/(\varepsilon_0 m_e)]^{1/2}$ and $\Omega_e = eB/m_e$ are, respectively, the e^- plasma and e^- cyclotron angular frequencies, $k_\parallel = N_\parallel \omega_0/c$ is the parallel wave vector, with e = electron charge, ε_0 = vacuum dielectric constant). Being $|D|/k_0 \approx \omega_{pe}/(\Omega_e k_\parallel)$ inversely proportional to B and directly proportional to the square root only of n_e, decreasing the magnetic field enhances the effect of the scattering on η_{CD} more than an equal relative density rise. Increasing n_e, then, counteracts only partially the beneficial influence of the toroidal $N_\parallel$ upshift, mentioned above, with the final result of the weak, yet positive, consequence on η_{CD}, given in equation (4). These arguments, however, do not presume to exhaust the possible effects of the edge plasma on the LH wave properties, as reported in [28].

The large discrepancy between the expected effect of the launched $N_{\parallel 0}$ on η_{CD} and that found, respectively, close to inverse square (equation (6)) and $\eta_{CD} \propto 1/N_{\parallel 0}^{0.3}$ (equation (4)) has prompted us to check the validity of this scaling law extending as much as possible the interval of $N_{\parallel 0}$. The

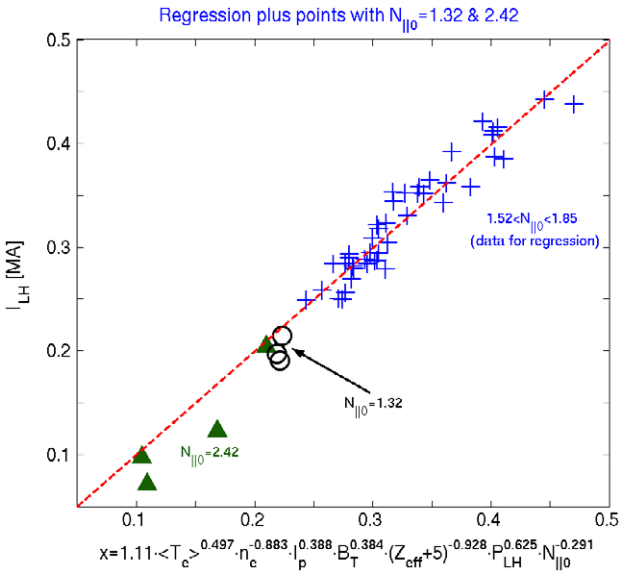

Figure 8. Discharges with $N_{\|0} = 1.32$ (○) and =2.42 (▲) compared with the regression laws and the related points used in figure 2. Despite the less driven current fraction the same scaling with $N_{\|0}$ holds.

regression analysis database, actually limited to cases with $N_{\|0} = 1.82$ and $= 1.52$ plus some combination of them, has then been supplemented with discharges having $N_{\|0} = 1.32$ and $= 2.42$. The accessibility criterion is still satisfied even for the lowest $N_{\|0}$, but the magnitudes of the residual V_{loop} are larger than that for the original data because of the low coupled power and small driven current fraction. However, the limited influence of the loop voltage, remarked above, gives sense to comparing the relevant estimates of I_{LH} with the rest of the data. This is shown in figure 8, where these points are plotted versus the abscissa calculated according to equation (3*a*) and are added to the data of figure 2. Within the error uncertainties the weak dependence of the overall driven current on the $N_{\|}$ spectrum, summarized by the relation $I_{\text{LH}} \propto 1/N_{\|0}^{0.3}$, is confirmed by these new points. The complex FTU situation makes it difficult to single out the relative weight of the different contributions to this fact. The edge scattering does play an important role again, because waves with smaller $N_{\|0}$ (i.e. smaller momentum) are scattered easier, but also the quite large poloidal spread of the LH launcher ($\pm 40^{\circ}$), with the associated large spread of the trajectories and toroidal $N_{\|}$ shifts and the actual absorption processes with the multiple wall reflections, can substantially modify the effective $N_{\|}$ spectrum. Significantly, indeed, the experimental values of η_{CD} approach the expected magnitude at high temperature (figure 4), where absorption needs a lower number of the reflection at the walls. The $N_{\|}$ spectral broadening caused by these two latter effects could be evaluated for each singular discharge by a full ray tracing and absorption code, but this great amount of work, if applied on a wide multi-shot data base as that considered here, is beyond the scope of the present work, finalized to give simple scaling laws.

Finally, the impurities behaviour concerning the CD efficiency is close to the expectations.

5. Effect of ECH absorption on electron tails

A separate section is needed to describe the effect of direct absorption of EC waves on the LH generated fast e^- tails. The EC power source in FTU (see table 1) has a frequency $f_{\text{EC}} = 140\,\text{GHz}$. The resonant magnetic field, defined by $2\pi f_{\text{EC}} = eB/m_e$, is $B_{\text{res}} = 5\,\text{T}$ for non-relativistic (cold) electrons. If resonance takes place only with the bulk electrons, which can be retained cold from the relativistic point of view, no peculiarity follows the injection of EC waves. Possible changes induced on the macroscopic plasma quantities, as the e^- temperature, can be included easily and consistently in those considered in the previous sections. Conversely, if the EC waves interact directly with the suprathermal e^- tail, new features should derive. The energy increment of the current carriers and the consequent decrease of collisionality should enhance the LHCD efficiency [30–32].

The resonance condition of the tail, which is supposed to travel at velocity $c/N_{\|\text{LH}}$, must take into account the relativistic mass increase and the Doppler effect due to a possible parallel velocity of the EC waves $v_{\|\text{EC}}$ (parallel index of refraction $n_{\|\text{EC}} = v_{\|\text{EC}}/|v_{\text{EC}}|$), and it is fixed now by [5]:

$$\frac{B_{\text{T}}(r)}{B_{\text{res}}} = \frac{N_{\|\text{LH}} - n_{\|\text{EC}}}{\sqrt{N_{\|\text{LH}}^2 - 1}}. \tag{7}$$

Here for the sake of clarity we added the suffix LH and EC to the parallel indices of refraction. The denominator in the rhs accounts for the relativistic mass increase, while the numerator accounts for the frequency shift observed by the fast electrons when the EC wave also possesses a parallel velocity. Among the several possible schemes for direct EC absorption by fast e^- tails, unambiguous results are attained only if the cold EC resonance is outside the plasma cross-section in order that bulk electrons play no role and if no direct current drive can be ascribed to the EC waves. The two requests imply, respectively, $B_{\text{T0}} \geqslant 6.8\,\text{T}$ and $n_{\|\text{EC}} \leqslant 0$. We confined our investigation to the case when B_{T0} ranges between 6.9 and 7.1 T and $n_{\|\text{EC}} = 0$, i.e. the EC waves are injected perpendicularly to B_{T}. This is the so-called downshifted regime (EC resonance frequency pushed down at $B =$ cost) where the e^- relativistic mass increment is balanced by an increase of B.

Synergetic effects have been already reported in FTU in previous works [4, 5] and subsequently confirmed on Tore Supra [33] and TRIAM-1M [34]. Both devices, however, operate in up-shifted regimes, where the Doppler shift ($n_{\|\text{EC}} > 0$) of the co-injected EC waves prevails on the relativistic mass increase, the cold EC resonance is retained inside the plasma and also some current is driven directly by the EC waves.

The multi-shot regression analysis revealed particularly suitable to highlight the synergy, both for the magnitude and for the circumstances where it takes place. The results are shown in figure 9, where the measured driven currents in the downshifted regime are plotted versus the regression variable of figure 2. Open circles are for the $N_{\|0} = 1.52$ case and full squares for $N_{\|0} = 1.82$, while crosses represent the original data. The latter incorporate all discharges with EC cold resonance in the plasma core that are not distinguishable in any way from the LH cases alone. In the downshifted

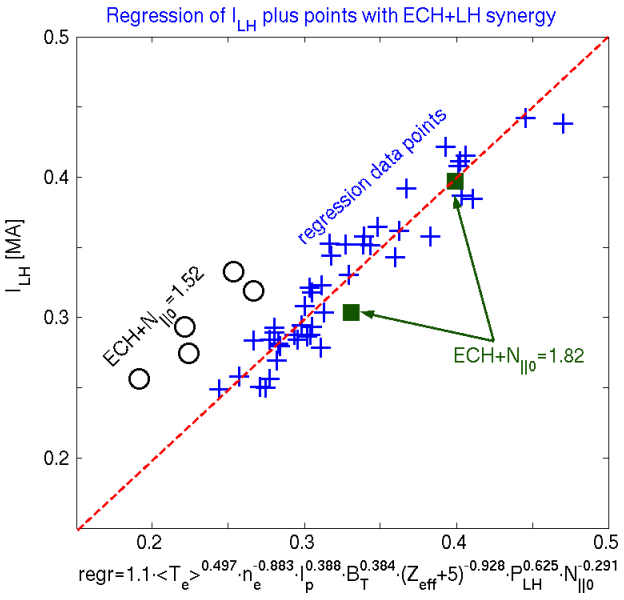

Figure 9. Total driven current in discharges with EC + LH waves and $B_{T0} = 7.1$ T. Synergy, i.e. a substantial enhancement of I_{LH} with respect to the discharges in figure 2 (+), is visible only for $N_{\|0} = 1.52$ (○). The independent variable is the same as in figure 2.

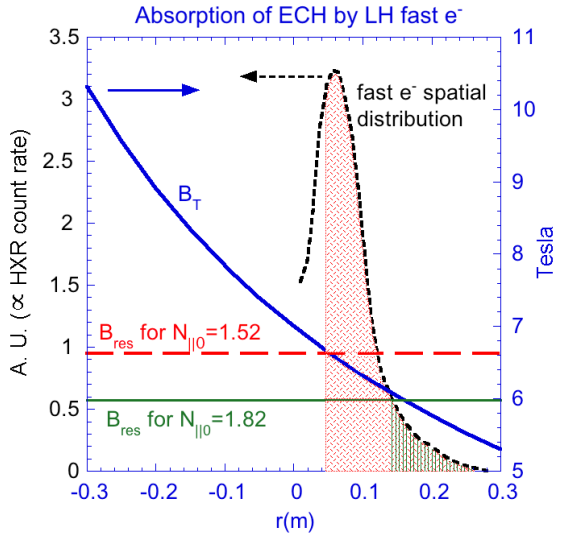

Figure 10. Distribution of the fast electron tails along the FTU minor radius, in arbitrary units. It is assumed proportional to the HXR perpendicular emission profile. The allowed interaction regions with EC waves are shown as shadowed areas, with dashes for the case $N_{\|0} = 1.52$ and lines for $N_{\|0} = 1.82$.

regime the amount of the driven current is considerably larger in the $N_{\|0} = 1.52$ case, whereas for $N_{\|0} = 1.82$ no increment is found. This is a consequence of the resonance condition equation (7), which fixes a precise radius for each electron speed. In particular for $B_{T0} = 7$ T, the velocities pertaining to the higher $N_{\|}$ would be resonant only at minor radii $r/a > 0.5$ approximately, where little or no LH power deposition occurs and hence no tails develop. Conversely, for $N_{\|} = 1.52$ resonance is possible up to $r/a \leqslant 0.2$ where most LH deposition also occurs. These statements are supported by the measured radial profiles of the hard x-rays (HXR) emitted perpendicularly to the magnetic field by bremsstrahlung of the LH generated fast electrons, in the energy interval 40–160 keV. The underlying assumption that these profiles reproduce faithfully the distribution of the fast e^- is valid if the radial diffusion of the latter is negligible during their lifetime. This holds already for plasma density lower than FTU [35] and becomes more and more valid as collisionality increases as in our case. The radial profile of the fast electron density so deduced, as in Tore Supra [36] and previously in FTU [6], is sketched in figure 10 for a discharge with $B_{T0} = 7$ T, in arbitrary units proportional to the count rate of the HXR detectors. The radial behaviour of $B_T(r)$ with the highest resonant field for the two spectra considered is also drawn. This limit is evaluated with the simplification that the high-energy tail is bounded on the high-speed side to $v_{max} = c/N_{\|0}$. Two different shadowings put into evidence, the integral area of the fast e^- population interested to direct absorption for the two diverse cases. Each population is bounded on the high field side by the resonance radius of its high speed, i.e. low $N_{\|}$, limit, since lower velocities need weaker B_T to balance the relativistic mass increase. The much larger number of electrons involved in the case $N_{\|0} = 1.52$ provides an explanation for the experimental finding. Estimates have been performed of the amount of the absorbed EC power and of the magnitude of the extra current due to the reduced e^- collisionality with the coefficients given in [31]. The density profile of the fast e^- carriers is taken from figure 10, properly scaled to give a total driven current of 0.35 MA. As a further simplifying assumption their perpendicular energy is considered negligible with respect to the parallel one. The result is a first pass absorption close to 18% for $N_{\|0} = 1.52$ and ≈1% for $N_{\|0} = 1.82$, with a total amount of current due to ECH waves of about 45 kA and 3.2 kA, respectively, to be compared with the experimental extra currents of 60–65 kA and 0 kA.

Remarkably, discharges with significant synergy EC-LH waves appear to follow the same scaling law obtained for the rest of the data but with a larger numerical factor. The relevant CD efficiencies are presented in figure 4 with the same graphical symbols. To our knowledge, the values found in synergy with ECH ($\eta^*_{CD} \approx 0.34$ [10^{20} m^{-2} A W]) are the highest so far reported in the tokamak literature. They are calculated taking into account only the total LH coupled power because EC waves do not have any parallel momentum and cannot directly drive any current, as is always done in all tokamaks when other heating systems are used in conjunction with LHCD.

6. Conclusions

The data set of the LHCD discharges is rich enough in FTU to allow a statistical analysis that has the aim of highlighting the factors determining the CD efficiency. The regression analysis technique has been carried out taking into account all the main quantities that can be either externally controlled or reliably measured in FTU.

The volume of the parameters space scanned is quite large and of direct interest for ITER. The line averaged density varies between 0.3 and 1.1 × 10^{20} m^{-3}, from values proper of most tokamaks to those relevant to ITER operations. The

volume averaged electron temperature ranges from 0.4 to approximately 1.2 keV, while its central value varies from ≈2 to 7.4 keV. The edge safety factor spans from 5 to 11, while the toroidal magnetic field from 5 to 7.2 T. Accessibility to the plasma core for the LH waves is good for all the discharges considered.

The regression analysis has pointed out the laws governing the LHCD efficiency and has allowed clarification of the reason for the large dispersion of the CD efficiency values so far found, not only when comparing different tokamaks but also within the data pertaining to a single device. The dependence of η_{CD} on the different quantities involved can be accounted for by considering the various physical processes involved, even though the analysis has not yet reached a quantitative level at the present knowledge of the plasma parameters.

The effect of increasing the electron temperature that enhances the CD efficiency, previously found [1], has been confirmed on a statistically more solid base. It is consistent with the picture that an electron tail must be formed extending on the low velocity side to the point to intercept the maxwellian distribution approximately at $v = 3.5\, v_{th}$, proposed in [26], and with the effects induced on the absorption process by T_e variations, as suggested in [27]. The increase of the efficiency as the discharge safety factor drops has been ascribed to the modifications suffered by the $N_{\|}$ spectrum as rays propagate in toroidal geometry. The slight increment of η_{CD} with density results from two counteracting processes: the beneficial one, due to propagation in toroidal plasmas, slightly dominates over the detrimental one, due to the enhanced wave scattering from the edge turbulence. The importance of the scattering due to edge density fluctuations is recognized also in the positive effect of increasing the magnetic field on η_{CD}.

Clear evidence of the synergy between the LH and EC waves is given, provided the EC power is directly absorbed on the fast e^- tails that must be located inside the resonance region, whose size is determined by the maximum e^- tail velocity. When these conditions are satisfied very high CD efficiency, close to 0.34 ($10^{20}\,m^{-2}\,A\,W^{-1}$), is obtained, the same as the largest ones so far quoted in the literature for JT-60U and JET, and for considerably hotter ($\langle T_e \rangle \approx 2$ keV) and less dense ($\bar{n}_e \approx 0.2 \times 10^{20}\,m^{-3}$) plasmas than in FTU.

Acknowledgments

The authors wish to thank all the people involved in managing the LH system for their precious and skilled assistance in every occasion, in particular, F. Mirizzi, M. Aquilini, S. Di Giovenale and P. Petrolini.

References

[1] Pericoli Ridolfini V. *et al* 1999 *Phys. Rev. Lett.* **82** 93–6
[2] Granucci G. *et al* 2004 *Fusion Sci. Technol.* **45** 387–401
[3] Gormezano C *et al* 2004 *Fusion Sci. Technol.* **45** 297–302
[4] Pericoli Ridolfini V. *et al* 2000 Combined LH and ECH experiments in the FTU tokamak *Proc. 18th Int. Conf. on Fusion Energy (Sorrento, Italy, 4–10 October 2000)* (Vienna: IAEA) CD-ROM file PDP7 and http://www.iaea.org/programmes/ripc/physics/fec2000/html/node1.htm
[5] Pericoli Ridolfini V. *et al* 2001 Synergy between LH and ECH waves in the FTU tokamak *AIP Conf. Proc. on Radiofrequency Power in Plasmas* vol 595, ed T K Mau and J deGrassie (Melville, New York: American Institute of Physics) pp 225–32 *(Proc. 14th Topical Conf. (Oxnard, CA, USA, 7–9 May 2001))*
[6] Barbato E. *et al* 2004 *Fusion Sci. Technol.* **45** 323–38
[7] Giruzzi G., Barbato E., Bernabei S. and Cardinali A. 1997 *Nucl. Fusion* **37** 673–80
[8] Itoh S. *et al* 1999 *Nucl. Fusion* **39** 1257–70
[9] Wesson J. 1997 *Tokamaks, Oxford Engineering Science Series N. 48* 2nd edn (Oxford: Clarendon) chapter 4.9
[10] Podda S. *et al* 2002 LH current drive at ITER relevant condition in FTU tokamak *Proc. 19th Int. Conf. on Fusion Energy (Lyon, France, 14–19 October 2002)* (Vienna: IAEA) CD-ROM file PD/P-07 and http://www.iaea.org/programmes/ripc/physics/fec2002/html/node470.htm#86935
[11] Fisch N.J. 1978 *Phys. Rev. Lett.* **41** 873–6
[12] Apicella M.L. *et al* 1997 *Nucl. Fusion* **37** 381–96
[13] Ekedahl A. *et al* 1996 Profile control in JET with off-axis lower hybrid current drive *Proc 23rd EPS Conf. on Plasma Physics and Controlled Fusion (Kiev, Ukraine)* vol 20C, Part II, pp 969–72
[14] Watari T. 1993 *Plasma Phys. Control. Fusion* **35** A63–76
[15] Porkolab M. 1984 *IEEE Trans. Plasma Sci.* **PS-12** 107
[16] Ushigusa K. *et al* 1989 *Nucl. Fusion* **29** 1052–5
[17] Naito O. and JT-60 team 1993 *Plasma Phys. Control. Fusion* **35** B215–22
[18] Rimini F.G. *et al* 1996 High power LHCD experiment in JET *AIP Conf. Proc. on Radiofrequency Power in Plasmas* vol 355 (Melville, New York: American Institute of Physics) pp 110–13 *(Proc. 11th Topical Conf. (Palm Springs, CA, USA, 17–19 May 1995))*
[19] Peysson Y. and the TORE SUPRA team 2000 *Plasma Phys. Control. Fusion* **42** B87–114
[20] Ikeda Y. *et al* 1995 *Proc. 15th Int. Conf. on Plasma Physics and Controlled Nuclear Fusion Research 1994 (Seville, 1994)* vol 1 (Vienna: IAEA) p 415
[21] Stevens J.E. *et al* 1988 *Nucl. Fusion* **28** 217–30
[22] Leuterer F. *et al* 1991 *Nucl. Fusion* **31** 2315–31
[23] Söldner F. 1995 *Annual Progress Report 1994 - LHCD* Memorandum of RF Division (Culham, UK: JET Joint Undertaking)
[24] Gormezano C. 2001 private communication (ENEA, C.R. Frascati)
[25] Pericoli Ridolfini V., Giannone L. and Bartiromo R. 1994 *Nucl. Fusion* **34** 469–81
[26] Barbato E. 1998 *Plasma Phys. Control. Fusion* **40** A63–76
[27] Takase H., Okano K. and Hatayama A. 1991 *Plasma Phys. Control. Fusion* **33** 749–62
[28] Cesario R., Cardinali A., Castaldo C., Paoletti F. and Mazon D. 2004 *Phys. Rev. Lett.* **92** 175002-1–4
[29] Barbato E. and Romanelli F. 1990 *Phys. Fluids* B **2** 2687–92
[30] Fidone I., Giruzzi G., Krivenski V., Mazzuccato E. and Ziebell L.F. 1987 *Nucl. Fusion* **27** 579–87
[31] Farina D. and Pozzoli R. 1989 *Phys. Fluids* B **1** 1042–8
[32] Dumont R.J. and Giruzzi G. 2004 *Phys. Plasmas* **11** 3449
[33] Giruzzi G. *et al* 2004 Synergy between Electron Cyclotron and Lower Hybrid Current Drive on Tore Supra *Proc. 20th Int. Conf. on Fusion Energy 2004 (Vilamoura, Portugal, 1–6 November 2004)* (Vienna: IAEA) CD-ROM file EX_P4-22, and http://www-naweb.iaea.org/napc/physics/fec/fec2004/datasets/EX_P4-22.html
[34] Zushi H. *et al* 2004 Overview of steady-state tokamak operation and current drive experiments in TRIAM-1M *Proc. 20th Int. Conf. on Fusion Energy 2004 (Vilamoura, Portugal, 1–6 November 2004)* (Vienna: IAEA) CD-ROM file OV_5-2 and http://www-naweb.iaea.org/napc/physics/fec/fec2004/datasets/OV_5-2.html
[35] Bartiromo R. *et al* 1993 *Nucl. Fusion* **33** 1483–92
[36] Peysson Y. 1999 Status of Lower Hybrid Current Drive *Proc. 13th Topical Conf. on Radiofrequency Power in Plasmas (Annapolis, USA 1999)* (New York: American Institute of Physics) pp 183–92